Formation of Composite Endothelial Cell–Mesenchymal Stem Cell Islets

A Novel Approach to Promote Islet Revascularization

Ulrika Johansson,[1] Ida Rasmusson,[1] Simone P. Niclou,[2] Naomi Forslund,[1] Linda Gustavsson,[1] Bo Nilsson,[1] Olle Korsgren,[1] and Peetra U. Magnusson[1]

OBJECTIVE—Mesenchymal stem cells (MSCs) contribute to endothelial cell (EC) migration by producing proteases, thereby paving the way into the tissues for ECs. MSCs were added to our previously described composite EC islets as a potential means to improve their capacity for islet angiogenesis.

RESEARCH DESIGN AND METHODS—Human islets were coated with primary human bone marrow–derived MSCs and dermal microvascular ECs. The capacity of ECs, with or without MSCs, to adhere to and grow into human islets was analyzed. The survival and functionality of these composite islets were evaluated in a dynamic perifusion assay, and their capacity for angiogenesis in vitro was assessed in a three-dimensional fibrin gel assay.

RESULTS—ECs proliferated after culture in MSC-conditioned medium, and MSCs improved the EC coverage threefold compared with EC islets alone. Islet survival in vitro and the functionality of the composite islets after culture were equal to those of control islets. The EC-MSC islets showed a twofold increase in total sprout formation compared with EC islets, and vascular sprouts emanating from the EC-MSC–islet surface showed migration of ECs into the islets and also into the surrounding matrix, either alone or in concert with MSCs.

CONCLUSIONS—EC proliferation, sprout formation, and ingrowth of ECs into the islets were enhanced by MSCs. The use of composite EC-MSC islets may have beneficial effects on revascularization and immune regulation. The technique presented allows for pretreatment of donor islets with recipient-derived ECs and MSCs as a means of improving islet engraftment.
Diabetes **57:2393–2401, 2008**

The islets of Langerhans are micro-organs, with afferent and efferent blood vessels connecting the capillary network of the islets to the circulation system (1). Intra-islet endothelial cells (ECs) are fenestrated, and the density of the capillary network in the islets is ~10 times higher than that of the surrounding exocrine tissue (2,3). During the process of islet isolation before transplantation, the ECs in the islets lose their external vascular support; this situation contributes to their dedifferentiation, apoptosis, and necrosis during subsequent in vitro culture (4).

The formation of new capillaries during revascularization is a complex process that involves digestion of the vascular wall by proteases and the migration, proliferation, and differentiation of ECs (5). When blood vessels are assembled, ECs produce platelet-derived growth factor, which attracts supportive cells, including mesenchymal stem cells (MSCs) that can differentiate into pericytes (6).

We hypothesized that adding MSCs to our previously described composite EC islets (7) might improve the adherence of the ECs to the islets and subsequent vascularization because MSCs contribute to EC migration by producing proteases, thereby paving the way into the surrounding tissue for the immature EC sprouts (8). MSCs have also been shown to upregulate the expression of angiopoietin and vascular endothelial growth factor (VEGF) in ECs, contributing to an increase in angiogenesis and stabilization of the vasculature (9). Moreover, MSCs have been shown to possess important immune-modulating properties (10), and they do not trigger adaptive immune reactions, which could make them ideal in islet transplantation setting (11,12).

The present study describes a gentle and reproducible technique for forming EC-MSC islets that is designed to take into consideration the inherent characteristics of the various cell types involved and to take advantage of the anchorage-dependent growth of ECs and MSCs. Our data demonstrate that addition of MSCs to our composite islets enhanced the capacity of ECs to enclose the islets without compromising the functionality of the islets. Importantly, the MSCs stimulated EC sprout formation not only into the surrounding matrices, but also into the islets where intra-islet capillary-like structures were formed.

RESEARCH DESIGN AND METHODS

Isolation of islets of Langerhans. Human islets of Langerhans were isolated at the Division of Clinical Immunology at Uppsala University by using a modified semi-automated digestion-filtration method, then cultured in CMRL-1066 with supplements (islet medium) (13–15).

Islets were released for research after approval by the ethics committee at Uppsala University Hospital. Pancreata from 20 donors were used (4–7 donors per experiment). The purity of the islet preparations was 75–95%, with the exception of one preparation that was 45% pure.

Cell culture. MSCs were isolated from human adult bone marrow as previously described (10). In brief, bone marrow was harvested from the iliac crest of adult volunteers (n = 8) after approval from the ethics committee at Huddinge University Hospital. The cells were classified as MSCs on the basis of their ability to differentiate into bone, fat, and cartilage and by flow cytometric analysis (positive for CD29, CD44, CD73, CD166, and CD105, but

From the [1]Division of Clinical Immunology, the Department of Oncology, Radiology and Clinical Immunology, Uppsala University, Uppsala, Sweden; and the [2]Centre de Recherche Public-Santé, NorLux Neuro-Oncology Laboratory, Val Fleuri, Luxembourg, Luxembourg.
Corresponding author: Ulrika Johansson, ulrika.johansson@klinimm.uu.se.
Received 15 July 2007 and accepted 23 May 2008.
Published ahead of print at http://diabetes.diabetesjournals.org on 2 June 2008. DOI: 10.2337/db07-0981.

See accompanying commentary, p. 2269.

negative for CD14, CD34, and CD45) and were used from passage 3-9 (FACScalibur; Becton Dickinson, Franklin Lakes, NJ). Potential EC contamination of the MSC population was assessed by flow cytometry (Becton Dickinson) ($n = 3$). The cells were stained for CD90 (1:100; BD Bioscience Pharmingen, San Diego, CA), the EC pan marker CD31 (1:100; Becton Dickinson), and the lectin Ulex europeaus agglutinin-1 (UEA-1, 1:100; Vector Laboratories, Peterborough, U.K.). Human dermal microvascular ECs HDMECs (PromoCell, Heidelberg, Germany) derived from adult dermis were cultured on 1% gelatin-coated flasks in EC Growth Medium Microvascular with supplements (EC medium; PromoCell). The ECs were used from passage 3-12.

Cell labeling. MSCs and ECs were labeled using CellTracker (CT) green and CT orange CMRA, respectively, according to the manufacturer's protocol (Molecular Probes, Eugene, OR).

Thymidine assay and coculture of cells. Thymidine assays were performed according to a standard proliferation protocol measuring [^{3}H]thymidine (1μCi/ml) incorporation (16). ECs were plated in 24-well plates, with 25×10^3 cells/well in EC medium with supplements for 24 h and then cultured in EC medium without supplements but containing 0.5% fetal bovine serum (starvation medium) for an additional 24 h (basal control) or stimulated with either VEGF-A (20 ng/ml; Peprotech, London, U.K.) in starvation medium or MSC-conditioned medium (supernatant from 24-h MSC cultures in starvation medium). [^{3}H]thymidine incorporation (at 20–24 h) was determined by liquid scintillation counting. Triplicate samples were assayed in three individual experiments. A mixture of 25×10^3 CT green–labeled MSCs and 25×10^3 CT orange–labeled ECs were cocultured in eight-well glass culture slides (Becton Dickinson) with EC medium and analyzed by fluorescence microscopy after 3 days.

Coating of islets of Langerhans with ECs and MSCs. Islets of Langerhans (10,000–30,000 islet equivalents) were incubated within 2–5 days after isolation with 0.5×10^6 CT orange–labeled ECs (EC islets) or with 0.25×10^6 CT green–labeled MSCs in combination with 0.25×10^6 CT orange–labeled ECs (EC-MSC islets) in a total volume of 500 μl. The cell suspensions were incubated at 37°C for 2–3 h in suspension culture tubes in EC medium and mixed gently twice per hour during the incubation. Thereafter, the EC islets, EC-MSC islets, and untreated control islets were cultured for up to 6 days at 37°C in EC medium or islet medium (CMRL; Invitrogen) until analyzed. The medium was changed every second day. Quantification of EC adherence was performed on EC islets and EC-MSC islets after 1 and 4 days of culture.

In vitro islet survival assay and cytokine and insulin content determination. A total of 100 islets per donor ($n = 6$) were hand picked: 50 islets were coated with 5×10^3 MSCs and 5×10^3 ECs, and 50 islets were untreated. All islets were cultured for 6 days in EC medium, with a medium change every second day. The number of remaining islets in the respective groups were counted after 1, 3, and 6 days of culture, and the islet number was confirmed after 6 days by dithizone staining (18). Control and EC-MSC islets were collected after 6 days of culture. Total DNA (Picogreen; Invitrogen), interleukin (IL)-8, IL-6 (R&D Systems, Oxford, U.K.), monocyte chemotactic protein-1 (MCP-1) (Serotec, Oxford, U.K.), tissue factor (TF) (Imubind; American Diagnostica, Stamford, CT), and insulin (Mercodia) contents were measured on a Gyrolab workstation (Gyros, Uppsala, Sweden), and the values were divided with total DNA. Four or more different islet isolations with 20 islets in each condition were analyzed.

Dynamic perifusion. The functionality of the islets coated with EC-MSC and of untreated islets from the same isolation was tested at different time points after coating (at 24 h and day 3–4). EC medium was used during the first 24 h of suspension culture; thereafter, the medium was changed to islet medium with supplements (17). Islets were challenged in a dynamic perifusion system, beginning with a low glucose concentration (1.67 mmol/l) during the first 36 min, followed by a high-glucose challenge (20 mmol/l) for 42 min, then reexposure to the low glucose concentration during the last 48 min. Fractions were collected at 6-min intervals over 126 min and analyzed for insulin content using commercial ELISA kits (Mercodia Insulin ELISA; Mercodia, Uppsala, Sweden). The area under the curve was calculated to evaluate the insulin secretion during high glucose stimulation with subtracted basal insulin secretion. Four different islet isolations with 20 islets in each condition were analyzed.

Fibrin gel in vitro angiogenesis assay. Control, EC, and EC-MSC islets were placed between two layers of fibrin gel (2.5 mg/ml fibrinogen and 2 μg/ml thrombin; Sigma-Aldrich, St. Louis, MO). After polymerization, EC medium supplemented with VEGF (30 ng/ml; Peprotech) was added. The islet preparations ($n = 6$) were cultured for 24 h, 48 h, and 3–4 days and then fixed in 4% paraformaldehyde. Sprouts were counted manually by the same person (blinded to the composition of the islet preparation), and 4–20 islets were counted per group in each experiment. The EC sprout length was measured using Leica Qwin software (Leica Microsystems, Nussloch, Germany) on pictures taken on day 4 of EC and EC-MSC islets in fibrin gel. The total EC sprout length per islet was calculated for each experiment (groups of 2–10 islets, $n = 6$). The mean total sprout length per islet for all the experiments ($n = 6$) was then calculated. The frequencies of the various sprout types were calculated by analyzing micrographs of EC-MSC islets from the fibrin gel experiments ($n = 6$).

Immunohistochemical staining. Composite and control islets were fixed in 4% paraformaldehyde for 30 min, washed in PBS, and incubated in 20% sucrose/PBS overnight at 4°C, then embedded in optimal cutting temperature medium (Tissue Tech; Sakura Finetek, Zoeterwoude, Netherlands), frozen, cryosectioned, and permeabilized in 0.3% Triton X-100/PBS for 15 min. Immunohistochemical staining was performed using guinea pig anti-human insulin (1:400; Fitzgerald Industries International, Concord, MA) followed by Alexa Fluor 488-labeled goat anti-rabbit (1:1,000; Molecular Probes) or Alexa Fluor 488–conjugated mouse anti-human CD31 (1:100; Becton Dickinson). Counterstaining was performed with DAPI (10 μg/ml; Sigma-Aldrich).

Production of DsRed-expressing lentiviral particles and lentiviral vector infection of ECs. Stocks of *Discosoma* species–derived red fluorescent (DsRed)–expressing lentiviral vectors (Lv-DsRed) were produced by cotransfection of three plasmids, the viral core packaging construct pCMVdeltaR8.74, the VSV-G envelope protein vector pMDG.2, and the transfer vector pRRLsin-PPThCMV-MCS-wpre containing DsRed cDNA (a gift of W.T. Hendriks), into human embryonic kidney 293T cells as previously described (19,20).

HDMECs at passage 3 were seeded onto 1% gelatin-coated six-well plates (1×10^5 cells/well; AH Diagnostics) and cultured for 48 h. Virus at a titer of 2×10^5 TU/ml Lv-DsRed was added to the subconfluent cells in combination with 2 μg/ml Sequa-Brene (Sigma-Aldrich) in EC medium. The plate was spun for 60 min during the Lv-DsRed infection of the ECs, and, thereafter, additional fresh medium was added to the cells. The DsRed ECs were then used in the long-term islet culture experiments according to the previously described protocol for coating of islets.

Image analysis and quantification. Coating, morphology, and sprout analyses were performed using confocal laser scanning microscopy (Zeiss LSM 510 Meta; Carl Zeiss International, Oberkochen, Germany) and/or fluorescence microscopy (Nikon Elipse E600, Nikon TS100; Nikon, Tokyo, Japan). Confocal z-stack images composed of 10 pictures were merged to produce a picture for use in analyzing EC adherence. Micrographs were analyzed using Leica Qwin software (Leica microsystems) to determine the surface area and total sprout length. The frequency of particular types of sprout composition was calculated from pictures using Adobe Photoshop software. Quantification of islet number was accomplished by the use of a stereomicroscope (Leica Microsystems), and pictures were analyzed using Adobe Photoshop software. Ingrowth of DsRed ECs into the islets was evaluated using confocal microscopy z-stack images, visualizing ECs at a defined depth of 30 μm into the islets after 3 or 6 days of culture, with a majority of samples being analyzed after 6 days. A defined distance of 30 μm from the islet surface was chosen to yield good confocal resolution. The presence of ECs was scored as 0–3, with 0 indicating the absence of ECs from the islet section and scores of 1–3 indicating a scarce (1), intermediate (2), or abundant (3) amount of ECs present.

Statistical analysis. Data are presented as means ± SEM. Mean values were compared using a two-tailed Wilcoxon test for paired data, with significance set at $P \leq 0.05$.

RESULTS

Interaction between ECs and MSCs. Before coculture, the purity of each cell population (EC and MSC) was assessed by fluorescence-activated cell sorter analysis. This analysis showed that the MSCs stained positive for the stem cell marker CD90 but were negative for the EC marker CD31 and did not bind the human EC lectin UEA-1 (Fig. 1*A*), indicating an absence of contaminating ECs. The ECs were negative for CD90 but were positive for CD31 and bound UEA-1 (Fig. 1*B*). MSC-conditioned medium induced an increase in EC proliferation, with the magnitude of the increase being similar to that produced by the addition of 20 ng/ml VEGF-A to the culture medium (Fig. 1*C*).

To analyze the potential cell growth effects by MSCs on ECs, we cocultured MSCs (CT green) and ECs (CT orange) in EC medium at defined cell densities for 3 days. Morphological analysis of these cultures showed that the cells grew either on top of each other or aligned with one another, indicating interactions between the cells (Fig.

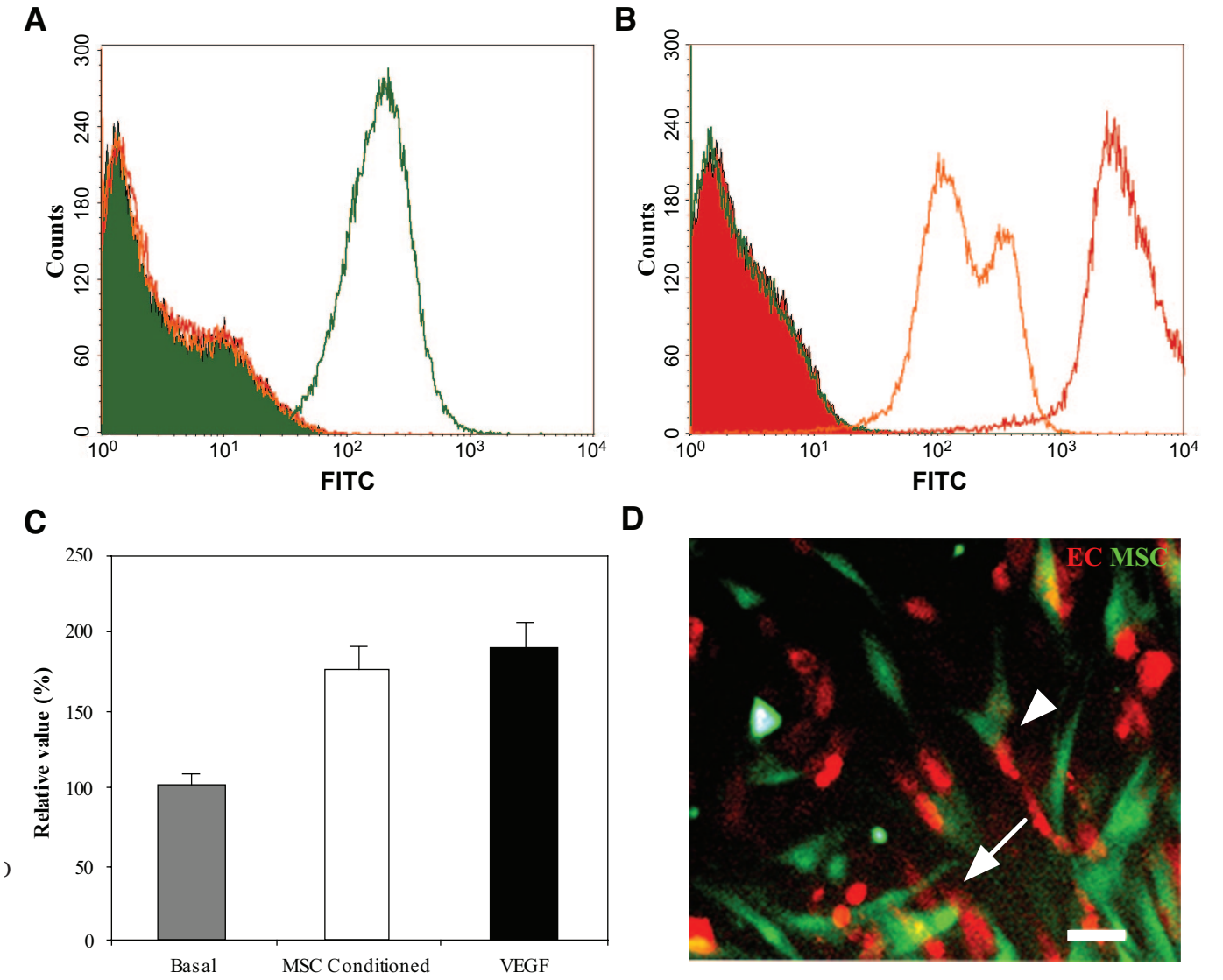

FIG. 1. Interactions between ECs and MSCs. Expression of CD90 (green line) and CD31 (orange line) and binding of UEA-1 (red line) to MSC (green, *A*) and EC (red, *B*), as assessed by flow cytometry (*A* and *B* show representative results of three experiments). *C*: EC proliferation in basal (gray), MSC-conditioned (white), or VEGF (black) medium. Results are expressed as the percentage of the basal response (means ± SEM) from three separate experiments performed in triplicate. *D*: Coculture of MSCs (green) and ECs (red). The cells grew either on top of one another (*D*, *arrow*) or aligned with each other (*D*, *arrowhead*). Scale bars = 50 μm. (Please see http://dx.doi.org/10.2337/db07-0981 for a high-quality digital representation of this figure.)

1*D*). Growth of ECs in double layers is an atypical phenomenon, indicating unusual growth interactions between the ECs and MSCs.

Improved islet coating by combining ECs and MSCs. ECs are adherent cells that interact with the extracellular matrix. We therefore evaluated the adherence of ECs (CT orange) and MSCs (CT green) to isolated islets. After 3-h incubation of islets and ECs (EC islets), a few ECs were found to adhere to the islet surface (Fig. 2*A*, *left panel*). Combining ECs and islets with MSCs (EC-MSC islets) had no apparent effect on the coating of the islets by ECs at this early time point (Fig. 2*A*, *right panel*). However, after only 1 day of incubation, a threefold increase in the islet surface covered by ECs was observed in the presence of MSCs, as compared with EC islets (Fig. 2*B*, quantification in Fig. 2*C*). Morphological characterization of the ECs adhering to the islet surface repeatedly showed that the ECs flattened out and aligned themselves with the surface of the islets in the presence of MSCs (Fig. 2*D*). Analyses of sectioned EC islets and EC-MSC islets stained for insulin showed ECs adhering to both insulin-positive and insulin-negative cells in the islet preparations after 24 h of incubation (Fig. 2*E*–*G*). After 4 days in suspension culture, there was a tendency toward a decrease in the islet surface area covered by ECs in both EC islets and EC-MSC islets; however, this difference did not reach statistical significance ($n = 6$; $P = 0.16$ and $P = 0.06$, respectively). A few cell clusters remained uncoated in all groups (Fig. 2*B*, *right panel*, *arrowheads*).

EC islet and EC-MSC islet survival and function. Islet loss during the process of coating was evaluated by incubation of 50 hand-picked islets with ECs and MSCs according to the coating protocol. No loss of islets was observed during the formation of EC-MSC islets; however, a gradual decrease of ~20% in islet number was observed in both groups during the 6-day culture period (Fig. 3*A*). Cytokine analysis showed insignificant differences in the levels of IL-6 (0.005 ± 0.005, 0.07 ± 0.06 pmol/μg DNA), IL-8 (0.3 ± 0.1, 0.9 ± 0.04 pmol/μg DNA), TF (0.1 ± 0.01, 0.3 ± 0.07 pmol/μg DNA) and MCP-1 (0.2 ± 0.2, 0.6 ± 0.1

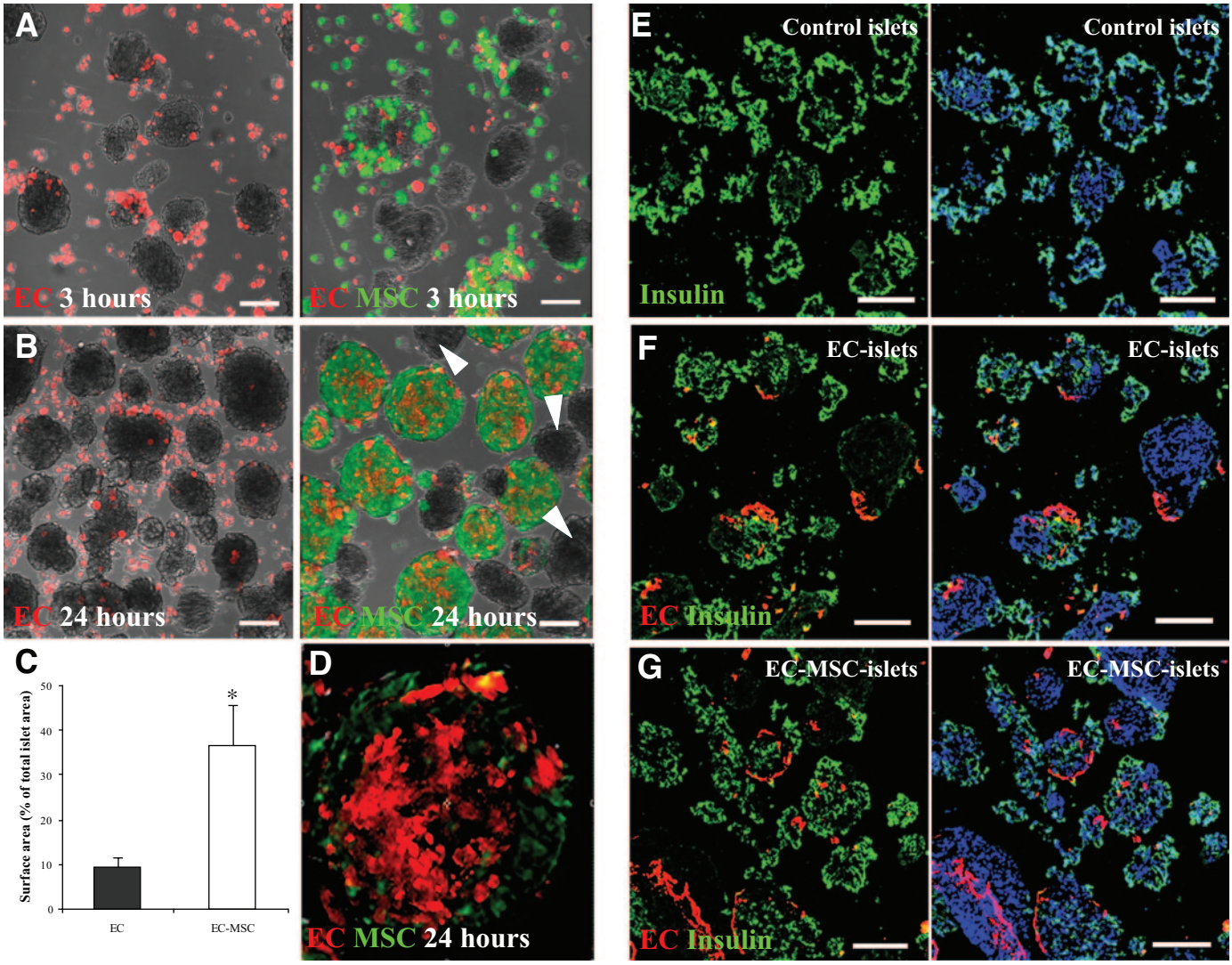

FIG. 2. Islet coating by ECs and MSCs. Islets were incubated with ECs (red; *A* and *B*, *left panel*) or ECs and MSCs (red and green, respectively; *A* and *B*, *right panel*) for 3 h (*A*) or 24 h (*B*). Some islets remained uncovered in all groups (*B*, *right panel*, *arrowheads*). EC adherence was quantified by calculating the surface area of digital micrographs of EC islets (black) and EC-MSC islets (white) (% of total islet area) after 1 day of culture (*C*) (means ± SEM; $n = 7$; *$P = 0.03$). ECs in the presence of MSCs were seen to flatten and coat the surface of the islets (*D*, enlarged islet from *B*, *right panel*). Insulin expression was determined by immunofluorescent staining of sectioned control islets (*E*), EC islets (*F*), and EC-MSC islets (*G*) after 24 h of culture. The images *E-G* show insulin (green), EC (red), and nuclear staining with DAPI (blue). Scale bars = 100 μm. (Please see http://dx.doi.org/10.2337/db07-0981 for a high-quality digital representation of this figure.)

pmol/μg DNA) in control islets and EC-MSC islets, respectively. The insulin content/DNA was 1.5 ± 0.4 ng insulin/ng DNA for the control islets and 0.9 ± 0.3 ng insulin/ng DNA for the EC-MSC islets on day 6.

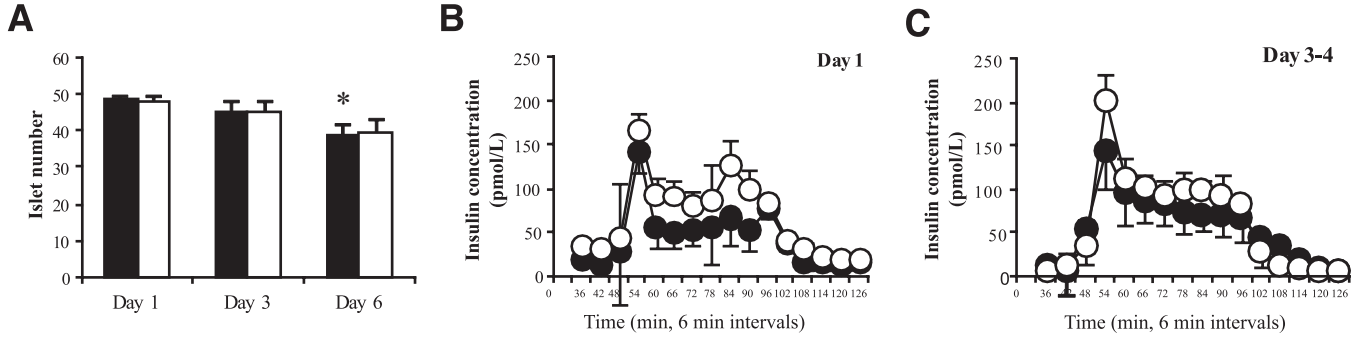

FIG. 3. Islet numbers, functionality, and dynamic insulin release of EC-MSC islets. Control islets (black) and EC-MSC islets (white) were counted after 1, 3, and 6 days (*A*) (mean of islet number ± SEM; $n = 6$; *$P = 0.03$; when the numbers of control islets on day 6 were compared with those of control islets on day 1). Insulin release was measured from control islets (black) and EC-MSC islets (white) cultured for 1 day (*B*) or 3–4 days (*C*). *B* and *C* show means ± SEM, $n = 4$.

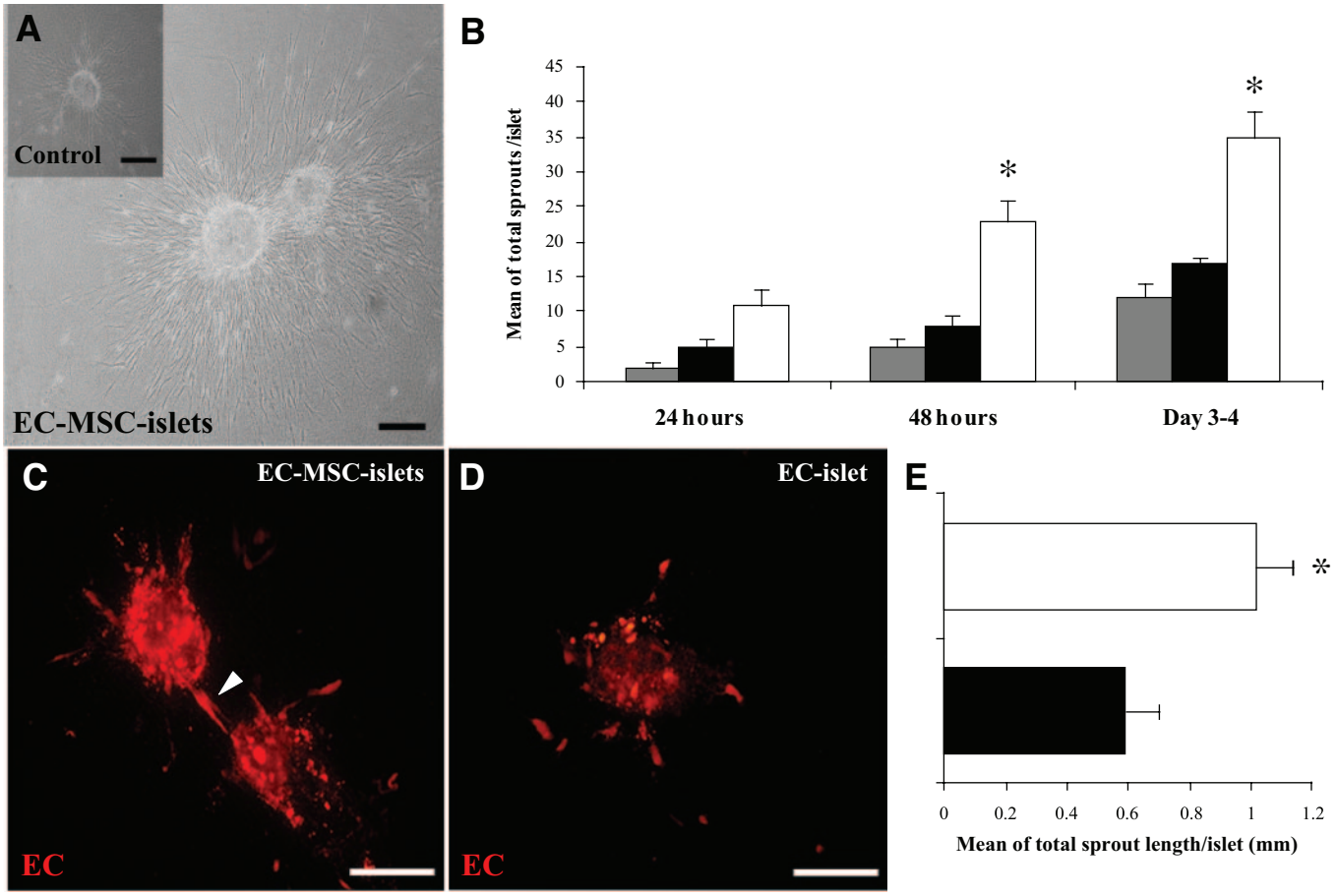

FIG. 4. Sprout formation in fibrin gels. Phase-contrast microscope images of control islets (*upper left corner*) and EC-MSC islets in fibrin gel after 4 days of culture (*A*). The number of sprouts per islet after 1–4 days in culture for control islets (gray), EC islets (black), and EC-MSC islets (white) (*B*) (mean of total sprout count ± SEM; $n = 6$; *$P = 0.03$; when EC-MSC islets were compared with control islets and EC islets at 48 h and 3-4 days). *C* and *D*: MSC-induced EC (red) with elongated sprouts in EC-MSC islets (*C*), as compared with EC-islets (*D*). *E*: EC sprout length measured in EC-MSC islets (white) and EC islets (black) (mean of total EC sprout length/islet ± SEM; $n = 6$; *$P = 0.03$). Scale bars = 100 μm. (Please see http://dx.doi.org/10.2337/db07-0981 for a high-quality digital representation of this figure.)

Insulin release by EC-MSC islets showed preserved dynamics during high-glucose stimulation after 1 and 3–4 days compared with control islets (Fig. 3*B–C*). No significant differences were seen in the stimulation indexes between control islets and EC-MSC islets at 1 day (5,090 ± 2,190 and 4,540 ± 1,300 pmol · min^{-1} · l^{-1}, respectively) or 3–4 days of culture (4,560 ± 1,330 and 5,090 ± 800 pmol · min^{-1} · l^{-1}, respectively).

Sprouting and invasion of fibrin gels. To evaluate the effect of angiogenesis, uncoated and coated islets were cultured in three-dimensional fibrin gels (Fig. 4*A* and *C–D*), in which ECs formed defined sprouts of patched ECs, and MSCs formed thin cords of aligned cells (21,22). After only 48 h, the total number of sprouts in the composite EC-MSC islets was higher than that in the control or EC islets. This difference remained after 3–4 days of culture (Fig. 4*B*).

When the islets came into close contact with each other, sprouts of ECs were formed between the EC-MSC islets, indicating paracrine stimulation (Fig. 4*C*, *arrowhead*). EC-MSC islets retained sprout formation over time, whereas in EC islets, the sprouts were disrupted and the ECs were separated from the islets (Fig. 4*C–D*). The median (± 1 quartile) EC sprout length in the EC-MSC islets was 900 μm (700–1,380 μm) and only 680 μm (300–840 μm) in the EC islets. Also, the total EC sprout length per islet was longer in the EC-MSC islets than in the EC islets (Fig. 4*E*).

Figure 5 shows the typical morphology of sprouts emanating from a composite EC-MSC islet after 2 days in culture. At this early stage, the sprouting was characterized by a complex course of events involving EC sprouts interacting with MSCs at the EC sprout base (Fig. 5*A*), ECs in close contact with MSCs (Fig. 5*B–C*), ECs at the leading tip of an MSC-initiated sprout (Fig. 5*D*), and MSCs at the leading tip of an EC sprout (Fig. 5*E*). ECs also migrated in groups to form a completely naked sprout with no apparent connection to the islet (Fig. 5*F*). Sprouts of ECs in close interaction with MSCs occurred twice as frequently as EC sprouts with nonaligned MSC cords. In the sprouts in which close cell interactions occurred between ECs and MSCs, there was a preference for ECs as the leading tip cells.

Vessel formation in islets coated with ECs and MSCs. After 24 h of culture in EC medium, the EC islets were stained for CD31 to reveal endogenous islet capillaries (Fig. 6*A*, *green*). An ingrowth of added ECs (CT orange) connecting to the native CD31-positive islet capillary network was frequently observed (Fig. 6*A*, *arrowheads*). To achieve a stable expression of DsRed, we infected the ECs with DsRed-labeled lentiviral particles. DsRed-infected ECs showed almost complete transduction after 2 weeks of culture, as visualized by merged phase-contrast and fluorescence microscopy images (Fig. 6*B*). The proliferative capacity of the DsRed EC in response to VEGF was unaffected (data not shown).

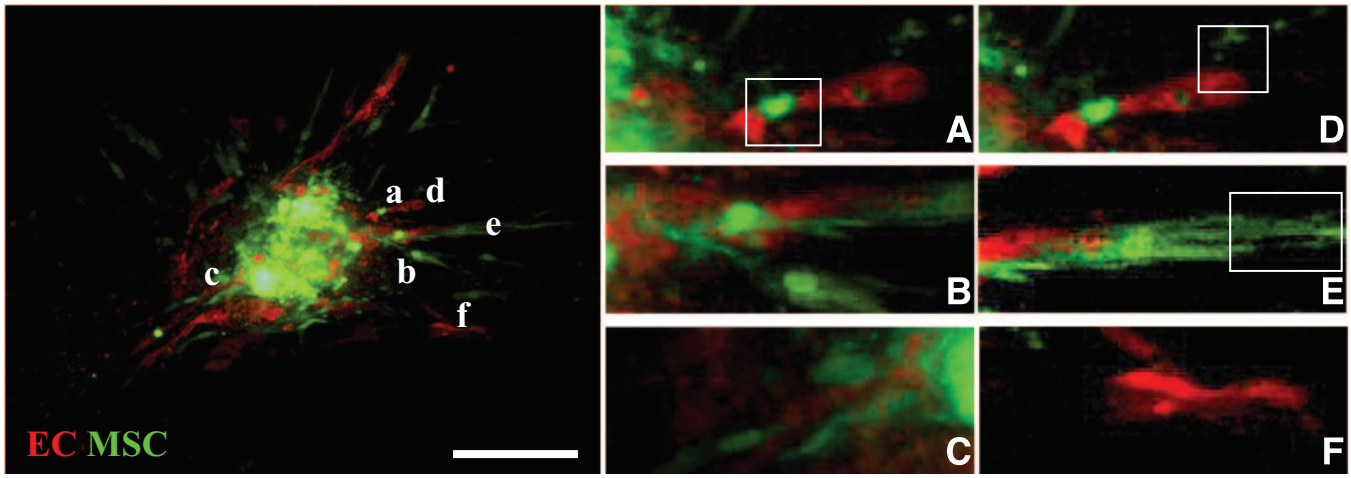

FIG. 5. Confocal scanning of sprout formation from composite islets with ECs and MSCs showing islets coated with MSC (green) and EC (red) cultured in three-dimensional fibrin gel (enlarged pictures to the right). *A–F*: MSCs at the base of an endothelial sprout (*A*), MSCs and ECs in close contact (*B*), ECs and MSCs growing side-by-side (*C*), an endothelial sprout tip (*D*), an MSC cord tip (*E*), and a naked, unconnected endothelial sprout (*F*). Scale bars = 100 μm. (Please see http://dx.doi.org/10.2337/db07-0981 for a high-quality digital representation of this figure.)

Confocal microscopy analyses of DsRed EC islets and DsRed EC-MSC islets after 6 days of suspension culture showed that the DsRed ECs had penetrated into the islets (Fig. 6*C*). Especially in the EC-MSC islets, the DsRed ECs had formed a dense network of capillary-like structures penetrating into the islets (Fig. 6*D*). The presence of DsRed ECs within the islets was scored at day 3 and 6. Whereas the EC islets had a mean score of 0.7 ± 0.2, the EC-MSC islets showed a higher level of penetration, with a mean score of 1.6 ± 0.4 (Fig. 6*E*). A comparison of the score distribution for the EC islets and EC-MSC islets showed that those with a score of 0 or 1 were predominantly EC islets, whereas the islets reaching a score of 2 or 3 were predominantly EC-MSC islets (Fig. 6*F*).

DISCUSSION

In the present study, modern tissue engineering was applied as a strategy to enhance the process of islet angiogenesis by combining ECs and supportive MSCs with isolated islets in culture. The capacity of the ECs to cover the islet surface was markedly enhanced by the presence of MSCs. This effect is most likely not only a result of enhanced adherence, but also a reflection of a change in the phenotype of the ECs that allowed them to stretch toward and interact with the islet surface, together with an increase in their proliferation. Importantly, in an established in vitro model of angiogenesis, the MSCs also stimulated EC sprout formation, not only into the surrounding matrices, but also into the islets where intra-islet capillary-like structures were formed.

Microvascular ECs were used to obtain an active EC phenotype with a capacity for angiogenesis that resembles a tentative future clinical situation involving harvesting autologous ECs from fat tissue (23). As compared with the aortic ECs that were used earlier (7), microvascular ECs are less covered by pericytes and, therefore, relatively more susceptible to remodeling (24). The relative capacity of EC populations to coat microcarrier surfaces is affected by the source from which they were obtained (25) and their expression of integrins, such as α5β 1, α1β 1, and αvβ 5. The same relationship, possibly reflecting variations in integrin expression (25), seems to hold true for their ability to coat islet surfaces (cf. [7]).

Established in vitro models of angiogenesis involve culturing ECs in three-dimensional polymers, such as fibrin or collagen gels (26,27). By using this model system, we were able to demonstrate the induction of sprout formation of ECs in the presence of MSCs, a response that could be monitored over time by confocal microscopy. Similarly, Ghajar and colleagues (8) have demonstrated stimulatory effects of MSCs on angiogenesis in three-dimensional fibrin gels. The induced vessel formation was due in part to degradation of the fibrin matrix by proteases produced by the MSCs, and sprout formation was enhanced even in matrices in which the matrix density was too high for the ECs to invade when cultured alone (8). This capacity of MSCs may be of particular importance in facilitating EC migration into dense micro-organs such as islets. In addition, MSCs most likely contributed growth factors and extracellular matrix production that serve to encourage the stabilization and maturation of the EC sprouts (9). This effect of MSCs was evidenced by the increased sprout formation by EC-MSC islets in fibrin gels, where close interactions between EC sprouts and MSCs occurred to a high degree. The MSCs express platelet-derived growth factor (PDGF) receptors and may respond to PDGF production by the ECs, leading to enhanced cell interactions (6,28). A majority of the EC sprouts that interacted closely with MSCs in the fibrin gel also showed a thicker sprout phenotype, suggesting that a maturation process occurred. In contrast, several of the sprouts emanating from the EC islets eventually collapsed and detached from their base at the islet surface.

Examination of sections of composite islets showed that the added ECs formed connections to the native islet capillaries. This growth of ECs into the islets was analyzed by scoring confocal microscopy z-stacks. A marked increase in the number of ECs growing into the islets was observed in the presence of MSCs. In these samples, the ECs formed capillary-like structures deep within the EC-MSC islets, indicating a prompt and enhanced angiogenic capacity.

The technique described here for forming EC-MSC islets has been designed to take into consideration the specific needs for in vitro support of the various cell types involved and to take advantage of the anchorage-dependent growth

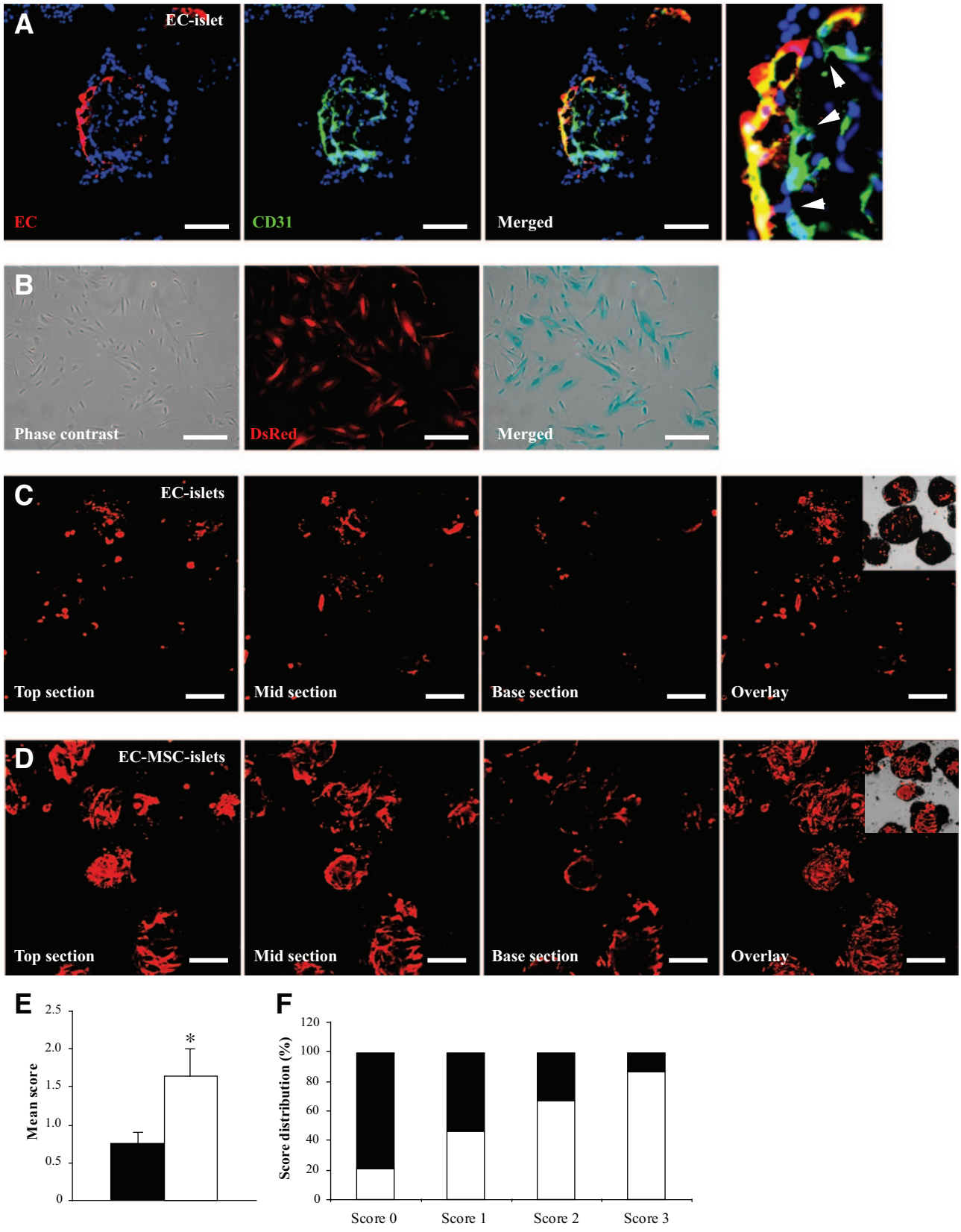

FIG. 6. Analysis of intra-islet vessel formation by accompanying ECs. Sectioned islets, coated with EC (red) and stained for CD31 (green), showed connections between accompanying EC and intra-islet capillaries (*A*, *arrowheads*). Yellow-colored vessels indicate CD31-positivity on added ECs. The last figure in panel *A* shows an enlargement of the connecting ECs. The merged phase-contrast and DsRed fluorescence microscope images/micrographs of infected human dermal microvascular ECs show an almost complete transduction efficiency with the DsRed lentiviral vector (*B*). *C* and *D*: DsRed ECs visualized in composite islets after 6 days of culture, EC islets alone (*C*), and EC islets in the presence of unlabeled MSCs (*D*). The insert in the last panel shows islets in bright-field with a DsRed EC overlay. Scale bars in *A* = 50 μm. Scale bars in *B–D* = 100 μm. Scoring of DsRed ECs in the islets showed an increased EC ingrowth in EC-MSC islets (white) compared with EC islets (black) (*E*) (mean score ± SEM; *n* = 7; **P* = 0.03). *F*: Score distribution for DsRed EC ingrowth into EC-MSC islets (white), as compared with EC islets (black). (Please see http://dx.doi.org/10.2337/db07-0981 for a high-quality digital representation of this figure.)

of ECs and MSCs. By utilizing the inherent characteristics of the different cell types, we were able to establish a gentle and reproducible technique. Most importantly, no additional loss of islets occurred during the formation of EC-MSC islets and their subsequent culture (6 days), when compared with untreated islets. A culture medium designed to support microvascular EC survival was applied to promote EC adhesion and proliferation on the islet surface unaffecting the islet function. Equally important is that the culture conditions applied did not promote the pro-inflammatory and procoagulant capacity of ECs (29,30), i.e, there was no difference in the level of expression of TF, IL-6, IL-8, or MCP-1 between the EC-MSC and control islets.

In the present communication, human ECs, MSCs, and islets were used. One limitation of this approach in the experimental setting is that evaluation of composite EC-MSC islet grafts in small animal models are not easily performed because of several significant species-specific differences in important areas such as angiogenesis, tissue repair, and innate immunity (31). Also, severely immunodeficient mice (SCID, nu/nu, and Rag) trigger strong innate immune responses that mainly target the vasculature of a transplanted organ due to the phylogenetic disparity between the two species, i.e., human-to-mouse is a discordant xenotransplantation model triggering activation of neutrophils, natural killer cells, macrophages, the complement and coagulation systems, and naturally occurring xenoreactive antibodies (32–39).

MSCs are currently being evaluated in clinical trials for their capacity to control severe graft-versus-host disease (40). Composite EC-MSC islet grafts could benefit from the immune regulatory effects of MSCs and from improved revascularization, thereby promoting transplantation at an extrahepatic site. This strategy requires a reliable source of recipient-derived ECs or endothelial precursor cells; however, human endothelial precursor cells can be obtained in relatively large numbers by sorting for circulating angiopoietin receptor Tie-2-positive cells (41) or from adipose-derived stem cells in human fat tissue (42,43). Our promising results with EC-MSC islets strongly suggest that they can contribute to the success of future clinical islet transplantation.

ACKNOWLEDGMENTS

This study was supported by grants from the Swedish Medical Research Council (K2005-72X-12219-09A and K2008-55X-12219-12-3), the Swedish Medical Research Council/Vinnova/Swedish Foundation for Strategic Research (60761701), the National Institutes of Health, the Novo Nordisk Foundation, Barndiabetesfonden, the Swedish Diabetes Association, and the Juvenile Diabetes Research Foundation.

The authors thank Daniel Brandhorst for assistance in statistical analysis, Deborah McClellan for editorial assistance, and the Nordic Network for Clinical Islet Transplantation for providing islet preparations.

REFERENCES

1. Bonner-Weir S, Orci L: New perspectives on the microvasculature of the islets of Langerhans in the rat. *Diabetes* 31:883–889, 1982
2. Henderson JR, Moss MC: A morphometric study of the endocrine and exocrine capillaries of the pancreas. *Q J Exp Physiol* 70:347–356, 1985
3. Kuroda M, Oka T, Oka Y, Yamochi T, Ohtsubo K, Mori S, Watanabe T, Machinami R, Ohnishi S: Colocalization of vascular endothelial growth factor (vascular permeability factor) and insulin in pancreatic islet cells. *J Clin Endocrinol Metab* 80:3196–3200, 1995
4. Giuliani M, Moritz W, Bodmer E, Dindo D, Kugelmeier P, Lehmann R, Gassmann M, Groscurth P, Weber M: Central necrosis in isolated hypoxic human pancreatic islets: evidence for postisolation ischemia. *Cell Transplant* 14:67–76, 2005
5. Conway EM, Collen D, Carmeliet P: Molecular mechanisms of blood vessel growth. *Cardiovasc Res* 49:507–521, 2001
6. Ball SG, Shuttleworth CA, Kielty CM: Mesenchymal stem cells and neovascularization: role of platelet-derived growth factor receptors. *J Cell Mol Med* 11:1012–1030, 2007
7. Johansson U, Elgue G, Nilsson B, Korsgren O: Composite islet-endothelial cell grafts: a novel approach to counteract innate immunity in islet transplantation. *Am J Transplant* 5:2632–2639, 2005
8. Ghajar CM, Blevins KS, Hughes CC, George SC, Putnam AJ: Mesenchymal stem cells enhance angiogenesis in mechanically viable prevascularized tissues via early matrix metalloproteinase upregulation. *Tissue Eng* 12: 2875–2888, 2006
9. Zacharek A, Chen J, Cui X, Li A, Li Y, Roberts C, Feng Y, Gao Q, Chopp M: Angiopoietin1/Tie2 and VEGF/Flk1 induced by MSC treatment amplifies angiogenesis and vascular stabilization after stroke. *J Cereb Blood Flow Metab* 27:1684–1691, 2007
10. Rasmusson I, Ringden O, Sundberg B, Le Blanc K: Mesenchymal stem cells inhibit lymphocyte proliferation by mitogens and alloantigens by different mechanisms. *Exp Cell Res* 305:33–41, 2005
11. Le Blanc K, Tammik C, Rosendahl K, Zetterberg E, Ringden O: HLA expression and immunologic properties of differentiated and undifferentiated mesenchymal stem cells. *Exp Hematol* 31:890–896, 2003
12. Maitra B, Szekely E, Gjini K, Laughlin MJ, Dennis J, Haynesworth SE, Koc ON: Human mesenchymal stem cells support unrelated donor hematopoietic stem cells and suppress T-cell activation. *Bone Marrow Transplant* 33:597–604, 2004
13. Ricordi C, Lacy PE, Finke EH, Olack BJ, Scharp DW: Automated method for isolation of human pancreatic islets. *Diabetes* 37:413–420, 1988
14. Brandhorst H, Brandhorst D, Brendel MD, Hering BJ, Bretzel RG: Assessment of intracellular insulin content during all steps of human islet isolation procedure. *Cell Transplant* 7:489–495, 1998
15. Lakey JR, Warnock GL, Shapiro AM, Korbutt GS, Ao Z, Kneteman NM, Rajotte RV: Intraductal collagenase delivery into the human pancreas using syringe loading or controlled perfusion. *Cell Transplant* 8:285–292, 1999
16. Cross MJ, Lu L, Magnusson P, Nyqvist D, Holmqvist K, Welsh M, Claesson-Welsh L: The Shb adaptor protein binds to tyrosine 766 in the FGFR-1 and regulates the Ras/MEK/MAPK pathway via FRS2 phosphorylation in endothelial cells. *Mol Biol Cell* 13:2881–2893, 2002
17. Johansson H, Goto M, Dufrane D, Siegbahn A, Elgue G, Gianello P, Korsgren O, Nilsson B: Low molecular weight dextran sulfate: a strong candidate drug to block IBMIR in clinical islet transplantation. *Am J Transplant* 6:305–312, 2006
18. Latif ZA, Noel J, Alejandro R: A simple method of staining fresh and cultured islets. *Transplantation* 45:827–830, 1988
19. Naldini L, Blomer U, Gallay P, Ory D, Mulligan R, Gage FH, Verma IM, Trono D: In vivo gene delivery and stable transduction of nondividing cells by a lentiviral vector. *Science* 272:263–267, 1996
20. Ruitenberg MJ, Plant GW, Christensen CL, Blits B, Niclou SP, Harvey AR, Boer GJ, Verhaagen J: Viral vector-mediated gene expression in olfactory ensheathing glia implants in the lesioned rat spinal cord. *Gene Ther* 9:135–146, 2002
21. Nakatsu MN, Sainson RC, Aoto JN, Taylor KL, Aitkenhead M, Perez-del-Pulgar S, Carpenter PM, Hughes CC: Angiogenic sprouting and capillary lumen formation modeled by human umbilical vein endothelial cells (HUVEC) in fibrin gels: the role of fibroblasts and Angiopoietin-1. *Microvasc Res* 66:102–112, 2003
22. Jakobsson L, Domogatskaya A, Tryggvason K, Edgar D, Claesson-Welsh L: Laminin deposition is dispensable for vasculogenesis but regulates blood vessel diameter independent of flow. *Faseb J* 22:1530–1539, 2007
23. Arts CH, de Groot P, Heijnen-Snyder GJ, Blankensteijn JD, Eikelboom BC, Slaper-Cortenbach IC: Application of a clinical grade CD34-mediated method for the enrichment of microvascular endothelial cells from fat tissue. *Cytotherapy* 6:30–42, 2004
24. Davis JS, Rueda BR, Spanel-Borowski K: Microvascular endothelial cells of the corpus luteum. *Reprod Biol Endocrinol* 1:89, 2003
25. Dietrich F, Lelkes PI: Fine-tuning of a three-dimensional microcarrier-based angiogenesis assay for the analysis of endothelial-mesenchymal cell co-cultures in fibrin and collagen gels. *Angiogenesis* 9:111–125, 2006
26. Hermant B, Desroches-Castan A, Dubessay ML, Prandini MH, Huber P,

Vittet D: Development of a one-step embryonic stem cell-based assay for the screening of sprouting angiogenesis. *BMC Biotechnol* 7:20, 2007
27. Jakobsson L, Kreuger J, Claesson-Welsh L: Building blood vessels–stem cell models in vascular biology. *J Cell Biol* 177:751–755, 2007
28. DiCorleto PE: Cellular mechanisms of atherogenesis. *Am J Hypertens* 6:314S–318S, 1993
29. Szotowski B, Antoniak S, Poller W, Schultheiss HP, Rauch U: Procoagulant soluble tissue factor is released from endothelial cells in response to inflammatory cytokines. *Circ Res* 96:1233–1239, 2005
30. Schouten M, Wiersinga WJ, Levi M, van der Poll T: Inflammation, endothelium, and coagulation in sepsis. *J Leukoc Biol*, 83:536–545, 2007
31. Ye Q, Murase N, Tanaka M, Demetris AJ, Manez R, McCauley J, Todo S, Starzl TE: Functional analysis of hamster kidney xenografts in the rat: possible functional incompatibility and adaptation of hamster kidney grafts in a xenogenic rat environment. *Transplant Proc* 28:694–695, 1996
32. Menger MD, Wolf B, Hobel R, Schorlemmer HU, Messmer K: Microvascular phenomena during pancreatic islet graft rejection. *Langenbecks Arch Chir* 376:214–221, 1991
33. Tanaka M, Murase N, Ye Q, Miyazaki W, Nomoto M, Miyazawa H, Manez R, Toyama Y, Demetris AJ, Todo S, Starzl TE: Effect of anticomplement agent K76 COOH on hamster-to-rat and guinea pig-to-rat heart xenotransplantation. *Transplantation* 62:681–688, 1996
34. Sachs DH: Mixed chimerism as an approach to transplantation tolerance. *Clin Immunol* 95:S63–S68, 2000
35. Lorant T, Krook H, Wilton J, Olausson M, Tufveson G, Korsgren O, Johnsson C: Intragraft cytokine mRNA expression in rejecting and non-rejecting vascularized xenografts. *Xenotransplantation* 10:311–324, 2003
36. Chandra AP, Salvaris E, Walters SN, Murray-Segal L, Gock H, Lehnert AM, Wong JK, Cowan PJ, d'Apice AJ, O'Connell PJ: Fate of alphaGal +/+ pancreatic islet grafts after transplantation into alphaGal knockout mice. *Xenotransplantation* 11:323–331, 2004
37. Bersztel A, Tufveson G, Gannedahl G, Johnsson C: A morphological sequential study of mouse-to-rat cardiac xenografts. *Scand J Immunol* 48:485–490, 1998
38. Sandrin MS, Vaughan HA, Dabkowski PL, McKenzie IF: Anti-pig IgM antibodies in human serum react predominantly with Gal(alpha 1–3)Gal epitopes. *Proc Natl Acad Sci U S A* 90:11391–11395, 1993
39. Tuso PJ, Cramer DV, Middleton YD, Kearns-Jonker M, Yasunaga C, Cosenza CA, Davis WC, Wu GD, Makowka L: Pig aortic endothelial cell antigens recognized by human IgM natural antibodies. *Transplantation* 56:651–655, 1993
40. Le Blanc K, Rasmusson I, Sundberg B, Gotherstrom C, Hassan M, Uzunel M, Ringden O: Treatment of severe acute graft-versus-host disease with third party haploidentical mesenchymal stem cells. *Lancet* 363:1439–1441, 2004
41. Vermehren D, Sumitran-Holgersson S: Isolation of precursor endothelial cells from peripheral blood for donor-specific crossmatching before organ transplantation. *Transplantation* 74:1479–1486, 2002
42. DiMuzio P, Tulenko T: Tissue engineering applications to vascular bypass graft development: the use of adipose-derived stem cells. *J Vasc Surg* 45:A99–A103, 2007
43. Zannettino AC, Paton S, Arthur A, Khor F, Itescu S, Gimble JM, Gronthos S: Multipotential human adipose-derived stromal stem cells exhibit a perivascular phenotype in vitro and in vivo. *J Cell Physiol* 214:413–421, 2008